DEVELOPMENT OF A MULTI-MODAL ELECTROCHEMICAL SENSING (MES) DEVICE FOR REAL-TIME MONITORING OF TUMOR MICROENVIRONMENT PARAMETERS IN CANCER IMMUNOTHERAPY

Jun Ying Tan¹, Malea Williams², Santosh Kumar Mandal², Anna Bottiglieri³, Aabila Tharzeen³, Rahul Sheth², Balasubramaniam Natarajan³, Punit Prakash³, and Jungkwun 'JK' Kim¹

¹Department of Electrical Engineering, University of North Texas, Denton, TX 76207, USA.
²Department of Interventional Radiology, University of Texas MD Anderson Cancer Center, Houston, TX 77065, USA.

³Department of Electrical and Computer Engineering, Kansas State University, Manhattan, KS 66506, USA.

ABSTRACT

This paper introduces a multi-modal electrochemical-based sensing (MES) device for real-time monitoring of the biophysical profile of the tumor microenvironment (TME). The MES device integrates pH, glucose, and impedance sensors onto microneedles. Characterization results show promising sensor performance. MES device performance was illustrated in an *in vivo* rat subcutaneous tumor model. This device holds the potential for informing pre-clinical studies of cancer immunotherapy by providing real-time TME insights, which may inform the assessment of candidate therapeutic approaches. Future work will explore additional sensors and further validation, paving the way for its use in research and pre-clinical studies.

KEYWORDS

Microsensors, electrochemical, real-time monitoring, pH, glucose, impedance sensors, microneedle.

INTRODUCTION

Immunotherapy is an emerging therapeutic approach for cancer treatment aiming at stimulating the body's immune system to target malignant tissues precisely [1]. The successful development of this approach hinges on high-quality pre-clinical studies supported by solid and well-researched data to ensure satisfactory efficacy in human patients [2]. However, diagnostics devices designed for small animals are extremely limited, with even scarcer availability of those with real-time monitoring capabilities. The absence of accessible tools for assessing small animal tumor microenvironment (TME) in pre-clinical studies has delayed the translation into clinical applications.

While magnetic resonance imaging (MRI) and micro-computed tomography (Micro-CT) scans are valuable tools for small animal TME assessment, offering detailed visualization as well as non-invasiveness [3], they are generally expensive and have limited availability. Furthermore, longitudinal studies in pre-clinical research for monitoring the post-treatment tumor response necessitate even more sophisticated system with fewer accessible options [3]. Histopathology or biopsy remains a common method for assessing TME, providing accurate diagnosis and comprehensive tumor characterization [4]. Still, the drawbacks, such as a limited number of possible diagnoses and the lack of real-time monitoring capabilities, constrain the potential for quantitative analysis [2].

This study aims to establish an alternative diagnostics tool for small animal TME assessment for research or preclinical studies by developing a compact, multi-modal

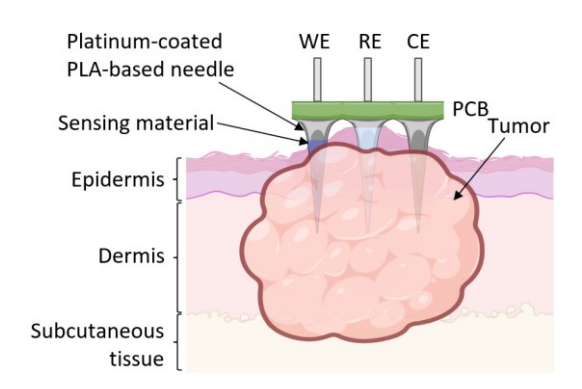


Figure 1: Conceptual drawing of the MES device applied to a tumor under skin.

electrochemical-based sensing (MES) device, as depicted in Figure 1. The MES device allows real-time monitoring of the TME, offering a versatile solution while reducing variability during longitudinal studies [2]. It comprises three functionalities: a primary working electrode (WE), a reference electrode (RE), and a counter electrode (CE). The working electrode is designed to support a range of sensors, including pH, glucose, and impedance sensors, facilitating a comprehensive assessment of the tumor microenvironment (TME). The functionality of each sensor has been evaluated, presenting an alternative TME diagnostics tool for small animals in pre-clinical studies.

FABRICATION PROCESS

Design of Microneedle

The design of the microneedle was determined based on the diameter of the tumor models in small animals (rats/mice), typically ranging from 2.4 to 14 mm as summarized in [5]. Hence, we tailored the prototype microneedles' height to 8 mm, suitable for accommodating most tumors. Nevertheless, it's worth noting that the microneedles' height and diameter remained adjustable, following the methods detailed in prior studies [6].

Fabrication of Microneedle

The microneedles were fabricated using diffraction lithography [6]. In brief, a photomask with a 3×3 array of circular photopatterns (D = 1.5 mm) was prepared then placed facing downwards on a resin tank filled with a photopolymer resin (Formlabs Inc., Surgical Guide Resin). A two-step UV exposure process was followed to form a high aspect ratio (height: base ratio > 5:1) microneedles using a broadband UV exposure system (OAI, Model 30, 200 to 450 nm). The first exposure was performed at an intensity of 20 mW/cm² for 1 min to form the

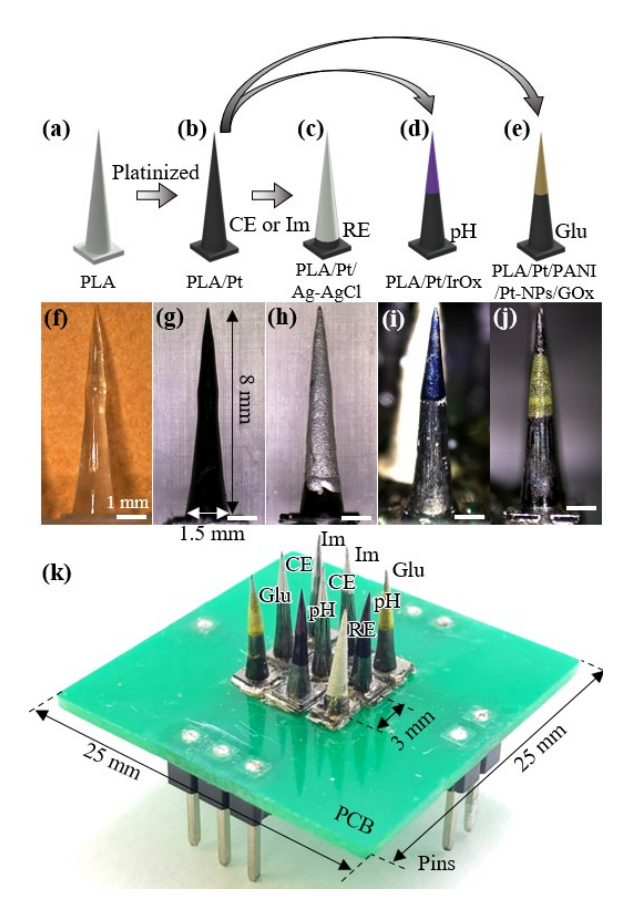


Figure 2: Fabrication process and results of the MES microneedles' body, then followed by a secondary exposure at 5 mW/cm² for another 1 min to form the sharp tips. The microneedles were carefully removed from the resin tank, developed in swirling isopropanol, and dried with compressed air. The 8-mm-tall microneedles were flood-exposed to UV light at 80 mW/cm² for 10 min to strengthen their mechanical stability. The photopolymer resin was selected for its high transmittance to UV light [7], enabling high aspect ratio microneedles, as demonstrated in the previous study [6]. The completed microneedle array was molded with Polydimethylsiloxane (PDMS) and then converted into Polylactic Acid (PLA) for biocompatibility and rigidity as shown in Figure 2(a, f).

Sensor Customization

For modifying the PLA microneedles to the counter electrode and impedance sensor, the microneedles were sensitized, and surface activated using oxygen plasma, then metalized using a DC sputter with 50-nm platinum for adhesion, followed by 300-nm copper seed layer for enabling electrical conduction. The copper thickness was increased to 5 µm through electroplating for improved conductivity. Lastly, it was coated with 100-nm platinum to be used as the CE and the impedance sensor in the MES device as shown in Figure 2(b, g). The platinized microneedle (PLA/Pt) also served as the foundation for further modification to satisfy various sensing capabilities.

Silver/Silver Chloride (Ag/AgCl) was selected as the surface modification for the RE. The platinized microneedle was treated with oxygen plasma, dip-coated in Ag/AgCl (60/40) screen-printing paste (Sigma Aldrich), then annealed at 60 °C in a convection oven for 30 min.

The coated microneedle was insulated with four layers of Nafion (5 wt. %) for biocompatibility, and prolonged potential stability as discussed in [8]. The completed RE (PLA/Pt/Ag-AgCl/Nafion) is depicted in Figure 2(c, h).

Iridium oxide (IrO₂) was selected as the surface modification for the pH sensor via an electrodeposition process onto the platinized microneedle, as described in [9]. A 100 ml solution was prepared by dissolving 0.15 g of iridium chloride, 1 ml of hydrogen peroxide (30 wt. %), and 0.5 g of oxalic acid sequentially, with at least 10 min of continuous magnetic stirring before the following reagent was added. The pH of the aqueous solution was adjusted to 10.5 by adding anhydrous potassium carbonate (K₂CO₃), while constantly monitored by a commercial pH meter (Orion Star A211, Thermo Fisher Scientific Inc.). The solution was left standing for stabilization for 48 hours. The electrodeposition process was performed with a threeelectrode system, including a commercial Ag/AgCl (in 3.8 M KCl) RE, the fabricated CE, and the platinized microneedle as the WE. IrO2 was electrodeposited onto the WE via cyclic-voltammetry (CV) with a potential sweep from -0.8 to 0.7 V for 100 cycles at a scan rate of 100 mV/s. Four layers of Nafion were dip-coated onto the IrO₂ surface for perm-selectivity, which prevents plaguing by common redox interferences while maintaining sensitivity to pH [9]. The completed pH sensor (PLA/Pt/IrO₂/Nafion) is shown in Figure 2(d, i).

For the glucose sensor, the platinized microneedle was electrodeposited with polyaniline (PANI) and platinum nanoparticles (Pt-NPs), then followed by drop-coating of glucose oxidase as described in [10]. The PANI electrodeposition solution was prepared with 100 mL of 0.1 M sulfuric acid (H₂SO₄) containing 40 mM aniline. The electrodeposition process of PANI was performed using CV with a three-electrode system, including a commercial Ag/AgCl (in 3.8 M KCl) RE, the fabricated CE, and the platinized microneedle as the WE. The potential was swept from -0.2 to 1.1 V at 50 mV/s for 20 cycles. Subsequently, Pt NPs were deposited using CV in 0.05 M hydrochloric acid (HCl) with 4 mM chloroplatinic acid (H₂PtCl₆) for 15 cycles with voltage sweeping from -0.6 to 0.8 V at 100 mV/s. The electrodeposited microneedle was carefully rinsed with deionized water and dried with compressed nitrogen. 10 µL of 8 mg/mL glucose oxidase (GOx) was drop-coated on the microneedle and allowed to dry at 4 °C for 12 hours. The microneedle was flipped over during the drying process so that the GOx would remain at the tip by gravity. The enzyme-coated microneedle was soaked in a 0.2% glutaraldehyde solution for 4 hours for enzyme immobilization and then carefully rinsed with deionized water. The completed glucose sensor (PLA/Pt/PANI/Pt-NPs/GOx) is shown in Figure 2(e, j).

Finally, on a 3×3 configuration of the MES device, one RE, two CE, two impedance sensors, two pH sensors, and two glucose sensors were soldered onto a printed circuit board (PCB) using silver epoxy to complete the MES device as shown in Figure 2(k).

CHARACTERIZATION AND RESULTS

All electrochemical measurements were performed by a potentiostat (Gamry Instruments, Reference 600+).

The fabricated RE was characterized with three

Ins. Mat.	Stable Potential	tential Stable Potential Time	
None (Ctrl)	$\text{-}6.03 \pm 0.15 \text{ mV}$	$12.53 \pm 1.01 \text{ min}$	
2-PDMS	$6.57 \pm 4.26 \; mV$	$15.42 \pm 4.08 \ min$	
2-Nafion	$\text{-}2.88 \pm 0.28 \text{ mV}$	$15.85 \pm 2.10 \text{ min}$	
4-Nafion	$-2.71 \pm 0.33 \text{ mV}$	15.36 ± 1.58 min	
Fabricated Ag/AgCI RE Potential vs. Commercial Ag/AgCI RE [mV] 2 0 10 21 0 0 0 0 0 0 0 0 0 0 0 0 0 0 0	No Insulation Two layers of PE Two layers of Na Four layers of Na 5 10 15 Time [min	offion Ag/AgCIRE Stable potential criteria 0 ± 5 mV	

Figure 3: Characterization results of Ag/AgCl reference electrode with various insulation layers.

insulation materials, including two layers of PDMS, two layers of Nafion, and four layers of Nafion coatings and one sample with no insulation material as the control. Three batches of RE were fabricated for each type of insulation material, resulting in a total of twelve REs. Open Circuit Potential (OCP) measurement was performed for each RE vs. a commercial Ag/AgCl RE probe in 3.8 M KCl solution for 30 min. The measured data were evaluated based on the stable potential after 30 min of OCP and the time required to reach 0 ± 5 mV vs. commercial RE, while the potential drift remained within 2 % margin after reaching a stable potential. The results were presented in Figure 3. The REs with no insulation material and two layers of PDMS coatings failed to reach 0 ± 5 mV after 30 min of OCP. REs with two and four layers of Nafion coatings showed comparable results, while the latter RE performed slightly better, achieving a stable potential of -2.71 ± 0.33 mV with a rapid stabilization time of 15.36 ± 1.58 min.

The characterization procedures for the impedance sensor were based on the reference [11], where conductivity was derived from impedance and expressed in terms of the electrode's cell constant and tissue conductivity, as shown in Equations 1 and 2. $Y = \frac{1}{Z} = G + j\omega C$

$$Y = \frac{1}{Z} = G + j\omega C \tag{1}$$

$$G = K \cdot \sigma \tag{2}$$

where Z is the impedance in ohms (Ω) , Y is the admittance in siemens (S), G is the conductance in siemens (S), C is the capacitance in farad (F), ω is the angular frequency in hertz (Hz), j is the imaginary unit $\sqrt{-1}$, σ is the conductivity of the tissue in siemens per meter (S/m) and K is the cell constant in per meter (m⁻¹). Sodium chloride (NaCl) solutions with seven concentrations, ranging from 0.001 to 0.15 M were prepared. Potentiostatic Impedance Electrochemical Spectroscopy measurement was performed in the solutions using a fourelectrode system, including two impedance sensors for

NaCl [M]	Conductivity [S·m ⁻¹]	Conductance [S]	Cell constant [m ⁻¹]
0.001	0.0124	0.000257	0.02084
0.005	0.0600	0.001239	0.02064
0.01	0.1175	0.002406	0.02048
0.03	0.3328	0.006684	0.02008
0.05	0.5323	0.010479	0.01969
0.1	0.9820	0.018950	0.01930
0.15	1.3780	0.026327	0.01911

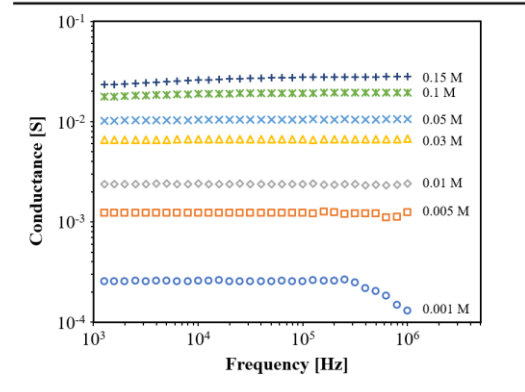


Figure 4: Impedance sensor characterization results.

voltage measurement and two counter electrodes for controlled current injection. The EIS measurement was measured from 1 kHz to 1 MHz, where the conductivity remains relatively constant as dielectric relaxation occurs in frequencies above 1 GHz [12]. The conductivity of the NaCl solution was derived from [13]. Figure 4 shows the characterization results of the impedance sensor, resulting in an average cell constant of 0.02 ± 0.00067 m⁻¹.

The pH sensor was examined in various pH buffer solutions, ranging from pH 4 to 10. OCP was measured using a three-electrode system for 180 s, and the results are shown in Figure 5(a). A sensitivity of -69.5 mV/pH with R² of 0.9935 was measured and a settling time of 60 seconds was observed, which is comparable to commercial pH meters that typically take 30 to 120 s to settle.

sensor glucose was evaluated chronoamperometry in glucose solutions with various concentrations, ranging from 2 to 6 mM, and the results are shown in Figure 5(b). A sensitivity of 0.71 µA/mM of glucose with R² of 0.9848 and an average settling time of 2 min were measured, offering the promising potential for real-time continuous local monitoring instead of the conventional one-time reading glucose meter.

The *in vivo* experimental study was approved by the Institutional Animal Care & Use Committee (IACUC) at the University of Texas MD Anderson Cancer Center. A total of three white male rats were included in this study. Cancer cells were cultured and injected into the animals' left and right legs and allowed to grow for two weeks. Animals were subjected to anesthesia before all experiments. A 16-gauge hypodermic needle was used along with a PCB with a 3×3 guide to create holes array in the skin. The MES device was inserted into the tumor via the holes array and attached to the animal's skin using skin glue. Figure 6(a) shows the MES device applied to a tumor in the animal's right leg. Figure 6(b) and (c) shows the ultrasound images of the tip and body of the sensors within the tumor with good structural integrity.

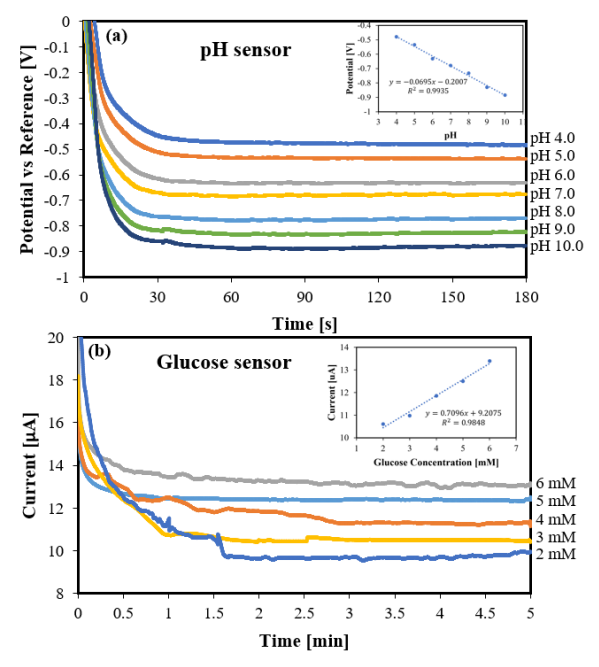


Figure 5: Characterization results of (a) pH and (b) glucose sensors.

CONCLUSIONS

This paper presents a multi-modal electrochemicalbased sensing (MES) device for real-time monitoring of essential TME parameters in experimental small-animal tumors. Three types of sensors, including impedance, pH, and glucose sensors have been successfully fabricated and characterized for the performance. The impedance sensor exhibited good conductance linearity across various concentrations and frequencies. The рΗ demonstrated a good sensitivity of -69.5 mV/pH with high linearity from pH 4 to 10 and a rapid 1-min settling time. The glucose sensor showcased a promising sensitivity of 0.71 μA/mM glucose with a practical 2-min settling time. Ultrasound images depicting successful tumor insertion were presented, showcasing no deformation of all nine electrode tips. While the characterization results were promising, further assessments, including in-vivo and exvivo testing, are essential to fully validate the reliability of the sensors.

ACKNOWLEDGEMENTS

The research was supported by the National Science Foundation (NSF) CNS 2039014, ECCS 2054567, ECCS 2029086, ECCS 2029077, and Korea Evaluation Institute of Industrial Technology (KEIT) 20018023.

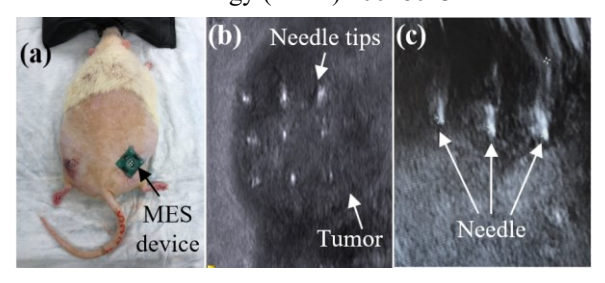


Figure 6: Insertion of the MES device to a tumor. (a) MES device applied to white rat's tumor. Ultrasound images of the (b) needle tips and (c) needle's body.

REFERENCES

- [1] H. Tang, J. Qiao, and Y. X. Fu, "Immunotherapy and tumor microenvironment," Cancer Letters, vol. 370, no. 1, pp. 85–90, Jan. 2016, doi: 10.1016/j.canlet.2015.10.009.
- [2] S. Budhu et al., "The importance of animal models in tumor immunity and immunotherapy," Current Opinion in Genetics & Development, vol. 24, pp. 46–51, Feb. 2014, doi: 10.1016/j.gde.2013.11.008.
- [3] M. Bilgen, "Feasibility and Merits of Performing Preclinical Imaging on Clinical Radiology and Nuclear Medicine Systems," Int J Mol Imaging, vol. 2013, p. 923823, 2013, doi: 10.1155/2013/923823.
- [4] M. A. Bjurlin et al., "Optimization of Prostate Biopsy: Review of Technique and Complications," Urologic Clinics, vol. 41, no. 2, pp. 299–313, May 2014, doi: 10.1016/j.ucl.2014.01.011.
- [5] L. A. Wirtzfeld et al., "A New Three-Dimensional Ultrasound Microimaging Technology for Preclinical Studies Using a Transgenic Prostate Cancer Mouse Model," Cancer Research, vol. 65, no. 14, pp. 6337– 6345, 2005, doi: 10.1158/0008-5472.CAN-05-0414.
- [6] J. Y. Tan et al., "Experimental Validation of Diffraction Lithography for Fabrication of Solid Microneedles," MDPI (Materials), vol. 15, no. 24, p. 8934, Dec. 2022, doi: 10.3390/ma15248934.
- [7] Formlabs, "Surgical Guide Resin Data Sheet." Accessed: Nov. 15, 2023. [Online]. Available: https://dental.formlabs.com/materials/#surgical-guide
- [8] L. Rivas et al., "Micro-needle implantable electrochemical oxygen sensor: ex-vivo and in-vivo studies," Biosensors and Bioelectronics, vol. 153, p. 112028, Apr. 2020, doi: 10.1016/j.bios.2020.112028.
- [9] K. Yamanaka, "Anodically Electrodeposited Iridium Oxide Films (AEIROF) from Alkaline Solutions for Electrochromic Display Devices," Jpn. J. Appl. Phys., vol. 28, no. 4R, p. 632, Apr. 1989, doi: 10.1143/JJAP.28.632.
- [10] J. Gao et al., "Simultaneous detection of glucose, uric acid and cholesterol using flexible microneedle electrode array-based biosensor and multi-channel portable electrochemical analyzer," Sensors and Actuators B: Chemical, vol. 287, pp. 102–110, May 2019, doi: 10.1016/j.snb.2019.02.020.
- [11] C. Gabriel, A. Peyman, and E. H. Grant, "Electrical conductivity of tissue at frequencies below 1 MHz," Phys Med Biol, vol. 54, no. 16, pp. 4863–4878, Aug. 2009, doi: 10.1088/0031-9155/54/16/002.
- [12] M. Chahbi et al., "A new approach to investigate the ionic conductivity of NaCl and KCl solutions via impedance spectroscopy," Materials Today: Proceedings, vol. 66, pp. 205–211, Jan. 2022, doi: 10.1016/j.matpr.2022.04.489.
- [13] P. Vanysek, "Equivalent Conductivity of Electrolytes in Aqueous Solution," in CRC Handbook of Chemistry and Physics, 99th Ed. (Rumble J. Ed.), CRC Press/Taylor & Francis, 2018.

CONTACT

*Jungkwun 'JK' Kim, tel: +1-940-369-7027; jungkwun.kim@unt.edu